ELSEVIER

Physica A 232 (1996) 349–368

PHYSICA A

Geometric criteria for phase transitions: The Ising model with nearest and next-nearest neighbor interactions☆

Borko D. Stošić[a,c,*], Srikanth Sastry[b], Dragan Kostić[c], Sava Milošević[d], H. Eugene Stanley[b]

[a] *Departamento de Física, Universidade Federal de Pernambuco, 50670-901 Recife-PE, Brazil*
[b] *Center for Polymer Studies and Department of Physics, Boston University, Boston, MA 02215, USA*
[c] *Institute for Nuclear Sciences, Vinča, P.O. Box 522, YU-11001 Belgrade, Yugoslavia*
[d] *Faculty of Physics, University of Belgrade, P.O. Box 550, YU-11001 Belgrade, Yugoslavia*

Received 24 May 1996

Abstract

We describe a geometric approach for studying phase transitions, based upon the analysis of the "density of states" (DOS) functions (exact partition functions) for finite Ising systems. This approach presents a complementary method to the standard Monte Carlo method, since with a single calculation of the density of states (which is independent of parameters and depends only on the topology of the system), the entire range of parameter values can be studied with minimal additional effort. We calculate the DOS functions for the nearest-neighbor (*nn*) Ising model in nonzero field for square lattices up to 12×12 spins, and for triangular lattices up to 12 spins in the base; this work significantly extends previous exact calculations of the partition function in nonzero field (8×8 spins for the square lattice). To recognize features of the DOS functions that correspond to phase transitions, we compare them with the DOS functions for the Ising chain and for the Ising model defined on a Sierpinski gasket. The DOS functions define a surface with respect to the dimensionless independent energy and magnetization variables; this surface is *convex* with respect to magnetization in the low-energy region for systems displaying a second-order phase transition. On the other hand, for systems for which there is no phase transition, the DOS surfaces are *concave*. We show that this geometrical property of the DOS functions is generally related to the existence of phase transitions, thereby providing a graphic tool for exploring various features of phase transitions. For each given temperature and field, we also define a "free energy surface", from which we obtain the most probable energy and magnetization. We test this method of free energy surfaces on Ising systems with both nearest-neighbor (J_1) and next-nearest-neighbor (J_2) interactions for various values of the ratio $R \equiv J_1/J_2$. For one particular choice, $R = -0.1$, we show how the "free energy surface" may be utilized to discern a first-order phase transition. We also carry out Monte Carlo simulations and compare these quantitatively with our results for the phase diagram.

* Corresponding author.

☆ This work is based in part on the Ph.D. thesis of S. Sastry.

PII S0378-4371(96)00239-7

1. Introduction

The two-dimensional Ising model in nonzero magnetic field remains one of the outstanding unsolved problems of modern statistical physics. Many properties of the model for different lattices and choices of the interaction parameters have been firmly established through a wide variety of approximate methods [1–5], and exact solutions have been obtained for special cases of interactions [6–8]. However, a straightforward procedure for establishing the existence, or absence, of phase transitions has not yet been established for systems with more than nearest-neighbor interactions.

Here we show that a study of the energy level degeneracies or density of states functions (DOS) for finite-size Ising systems provides a general geometric tool for discerning the existence of ordered phases, frustrated states and limits of phase stability. This method can be applied to a variety of interactions and lattice geometries. The DOS functions of finite Ising systems have been calculated on the triangular lattice in zero field, and the square lattice in both zero and nonzero field [9]. The DOS functions for finite lattices capture some of the basic properties of the infinite systems and, when scaled with the system size, show surprisingly regular behavior. The thermodynamic quantities calculated from them display the expected finite size scaling behavior already for very small system sizes.

We calculate the exact DOS functions for nearest-neighbor Ising systems in nonzero field on various lattice geometries. By comparing the DOS functions for different lattices, we find that the DOS surfaces are *convex* (with respect to magnetization [10], around zero magnetization) in the low-energy region for lattices with a phase transition at nonzero temperature. For lattices with no phase transition, the DOS surfaces are *concave*. This property of the DOS functions is directly related to the number of spin configurations with finite magnetization that can be realized at some given low-energy value. If the DOS surface is convex, the system is unlikely to be found in spin configurations having low values of the magnetization *and* low energies (so it exhibits nonzero equilibrium magnetization at low T). Conversely, if the DOS surface is concave, the system is most likely to be found in spin configurations with zero magnetization (so the equilibrium magnetization is zero for all T).

We extend the analysis to a quantitative study of properties by looking for dominant contributions to the partition function at different temperatures. We show that below the critical temperature T_c, a modification of the DOS surface (that can be related to the system free energy) has two distinct peaks corresponding to positive and negative spontaneous magnetization values. On the other hand, above T_c there is just one peak at zero spontaneous magnetization. In the more complicated case with both nearest-neighbor (*nn*) interactions J_1 and next-nearest-neighbor (*nnn*) interactions J_2, we show (by looking at the corresponding DOS surfaces) the existence of a first-order phase transition and discuss the behavior of the model for different signs and values of the ratio $R \equiv J_1/J_2$. We use this procedure to obtain the phase diagram for a specific choice of R and compare this phase diagram with the phase diagram we obtain by Monte Carlo simulations.

This paper is organized as follows. In Section 2 we explain the DOS function approach, while in Section 3 we present the results for the square and triangular lattices, Ising chain and the Sierpinski gasket. In Section 4 we treat the *nnn* Ising model, and explore the effect of different signs and values of the interaction ratio R. We summarize the results in Section 5.

2. The DOS functions

2.1. Definitions

First we outline the density of states formalism and establish the notation we shall follow subsequently. For simplicity, we treat here only the *nn* case. The generalization of the formalism to the more complicated *nnn* case is given is Section 4. The Ising Hamiltonian is given by

$$\mathscr{H} = -J \sum_{\langle nn \rangle} s_i s_j - H \sum_i s_i \,, \tag{1}$$

where J is the nearest-neighbor interaction strength, $s_i = \pm 1$ is the Ising spin variable at the site i, H is the external magnetic field, and $\langle nn \rangle$ denotes summation over the nearest-neighbor pairs. When $J > 0$ the energy contribution of a pair of parallel spins is lower (we say that the bond between them is "satisfied"). When $J < 0$ (antiferromagnetic case) the energy contribution of a pair of antiparallel spins is lower.

For any finite Ising system with arbitrary geometry, the energy spectrum is discrete. When $J > 0$, the ground state has all the bonds satisfied, with all the spins parallel to the field. Starting from the ground state configuration, the higher energy levels are obtained by flipping spins, so that more and more bonds are unsatisfied, and more spins are antiparallel to the field. The partition function of a ferromagnet with arbitrary geometry, composed of N spins interconnected by N_B bonds, can thus be written in the form [9]

$$Z = e^{\beta(JN_B + HN)} \sum_{k=0}^{N_B} \sum_{\ell=0}^{N} \mathscr{D}_{k\ell} e^{-2\beta(kJ + \ell H)} \,. \tag{2}$$

Here, $\mathscr{D}_{k\ell}$ are degeneracies of the discrete energy levels

$$E_{k\ell} \equiv J(-N_B + 2k) + H(-N + 2\ell) \,, \tag{3}$$

and β is the reciprocal of the temperature times the Boltzmann constant, $\beta \equiv 1/k_B T$. The first term on the right-hand side of (3) corresponds to the interaction energy of the system, while the second term represents the energy due to the external field H. The integer k $(0 \leqslant k \leqslant N_B)$ represents the number of unsatisfied bonds, and ℓ $(0 \leqslant \ell \leqslant N)$ the number of spins antiparallel to the field.

Expression (2) has been used in classic textbooks [11] to stress the fact that although the partition function depends on 2^N configurations, each of which is specified by N numbers $\{s_1, s_2, \ldots, s_N\}$, the energy of a configuration depends only on two numbers,

k and ℓ, and that the energy levels are in general highly degenerate. For example, the 10×10 square lattice with open boundary conditions has altogether $2^{100} \sim 10^{30}$ possible configurations, but only $(N_B + 1)(N + 1) = 18\,281 \sim 10^4$ different energy levels. Even with the largest computer, 10^{30} is too many calculations, but managing a polynomial with 10^4 terms is practicable. The main problem is thus to determine the degeneracy matrix $\mathscr{D}_{k\ell}$.

2.2. Convergence of the DOS function

Two decades ago the set $\mathscr{D}_{k\ell}$ was calculated [12] for the 5×5 square lattice and the $3 \times 3 \times 3$ cubic lattice, and the set $\mathscr{D}_k \equiv \sum_{\ell=0}^{N} \mathscr{D}_{k\ell}$ (for the zero field case) was calculated [13] using the transfer matrix (TM) method for the cubic $3 \times 3 \times 6$ lattice. The set $\mathscr{D}_k$ for the $5 \times 4 \times 5$ lattice was only recently calculated [14] using the TM method on the massively parallel Connection Machine CM II. The sets of degeneracies were used to calculate the thermodynamic response functions and the distributions of zeros of the partition function in the complex plane [12–15]. In Ref. [9] where the calculation of the set $\mathscr{D}_{k\ell}$ for the 8×8 square lattice was reported, it was shown that the sets $\mathscr{D}_{k\ell}$ can be regarded in their own right as relevant quantities for determining thermodynamic behavior of infinite systems.

We show how these degeneracies for different lattices form three-dimensional surfaces which converge rapidly with increasing system size towards definite shapes. Denoting the density of states by $\mathscr{D}(E,N)$, for a given system size N and a given energy value E, the relation

$$\ln \mathscr{D}(E,N) \sim N f\left(\frac{E}{N}\right) \tag{4}$$

holds for already very small systems [9]. The quantities

$$S_{k\ell} \equiv \frac{\ln \mathscr{D}_{k\ell}}{N_B}, \tag{5}$$

as a function of dimensionless scaled variables $\tilde{k} \equiv k/N_B$ $(0 \leqslant \tilde{k} \leqslant 1)$ and $\tilde{\ell} \equiv \ell/N$ $(0 \leqslant \tilde{\ell} \leqslant 1)$, with increasing system size, become independent of the system size and shape with a correction term of the order $\mathscr{O}(1/N_B)$. We shall use the term DOS function to describe the set $\{S_{k\ell}\}$, where $k = 1,2,\ldots,N_B$ and $\ell = 1,2,\ldots,N$. We shall denote the interaction energy scale and the magnetization scale by $\tilde{k}$ and $\tilde{\ell}$. We discuss the convergence of the DOS functions further in Section 3, where the results for the *nn* Ising model are presented.

2.3. The "free energy surface"

We introduce the "free energy surface" $F_{k\ell}$ per bond associated with the energy level $E_{k\ell}$ by the relation

$$Z = \sum_{k=0}^{N_B} \sum_{\ell=0}^{N} \exp(-\beta F_{k\ell} N_B), \tag{6}$$

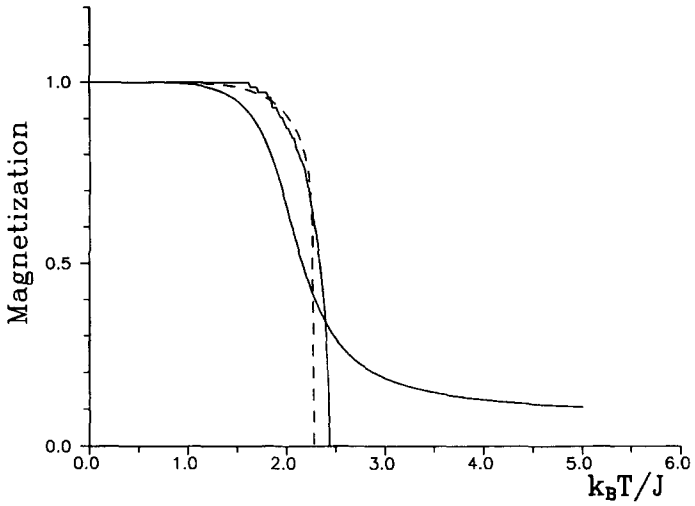

Fig. 1. The equilibrium magnetization (dashed line) of the infinite 2D Ising system [1], together with the average magnetization (solid line) of the 12×12 square lattice Ising system, and its net magnetization of the most probable states (the step-like curve). Compared to average magnetization, the net magnetization of the most probable states provides a better representation of the infinite system behavior.

where, from (3) and (5),

$$F_{k\ell} \equiv E_{k\ell} - k_B T S_{k\ell} \,. \tag{7}$$

We see that for the energy level $E_{k\ell}$, $S_{k\ell}$ and $F_{k\ell}$ define quantities analogous to the entropy and free energy. It should be stressed here that the DOS function depends *only* on the topology of the lattice, and not on the particular choice of temperature, field and value of the interaction parameter. Given the rapid convergence of the DOS surfaces (with respect to scaled energy and magnetization variables) towards the corresponding infinite system surface [9], the properties of the infinite system are approximated closely by the most probable configurations of the finite system at given values of temperature and field. We determine the most favorable (equilibrium state) region of interaction energy and magnetization for given values of temperature and field by studying the free energy surface. To this end, it is useful to rewrite expression (6) in the form

$$Z = e^{\beta(JN_B+HN)} \sum_{k=0}^{N_B} \sum_{\ell=0}^{N} \exp\left\{ N_B \left[-2\beta \left(\tilde{k}J + \tilde{\ell} \frac{N}{N_B} H \right) + S_{k\ell} \right] \right\}. \tag{8}$$

To determine the equilibrium interaction energy and magnetization values (for given T and H) one must subtract from the DOS surface $S_{k\ell}$ the plane $-2\beta(\tilde{k}J + \tilde{\ell}(N/N_B)H)$, and search for values of $\tilde{k}$ and $\tilde{\ell}$ for which the resulting surface $-\beta F_{k\ell}$ has the maximum value. Thus, we assume that we can represent the equilibrium state parameters by the corresponding values of the most probable state of the finite-size system. To corroborate this assumption, in Fig. 1 we present the equilibrium magnetization of the infinite 2D Ising system [1], together with the average magnetization of the 12×12

square lattice Ising system and the net magnetization of the most probable states. We see that the latter is a much better representation of the infinite system behavior.

Note that the DOS function calculated for the ferromagnetic system also describes the antiferromagnetic system, if the beginning and the end of the $\tilde{k}$ axis are interchanged (an unsatisfied bond in the ferromagnetic case is satisfied in the antiferromagnet). Thus, the part of the DOS function with $0 \leqslant \tilde{k} \leqslant 0.5$ corresponds to possible states of a ferromagnet, while the $1 \geqslant \tilde{k} \geqslant 0.5$ part corresponds to the antiferromagnetic states (negative temperatures).

3. Comparison between the DOS functions of Euclidean and fractal lattices

Next we compare the DOS functions of the *nn* Ising model in a field for different lattices: square, triangular, one-dimensional chain, and the Sierpinski gasket. This comparison enables us to draw a general conclusion about the relation between the concavity of the DOS surface and the existence of a phase transition. We describe briefly below how the DOS functions presented in this paper are calculated.

3.1. Euclidean lattices

In the case of 2D lattices with Euclidean geometry (such as the square and the triangular lattice), the DOS functions can be calculated by the TM method, introduced by Binder [13] (for the $H = 0$ case) and generalized in Ref. [9] (for the case $H \neq 0$). Using the TM method we have been able to extend [16] results for the exact DOS functions for square lattices up to 12×12 spins, and to calculate these functions for equilateral wedges of the triangular lattice up to 12 spins in the base. The DOS functions for the Ising chain are readily obtained for arbitrary system size from the known exact solution [2].

3.2. The Sierpinski gasket

In the case of the Sierpinski gasket the most efficient way of obtaining the DOS functions is by the real space renormalization group (RG) method [17,18], which we describe here briefly. The Sierpinski gasket can be obtained from an equilateral triangle (called generator) that contains four smaller identical unit triangles. The entire fractal lattice is constructed in self-similar successive stages, labeled by the integer n ($0 \leqslant n \leqslant \infty$), so that $n = 0$ and $n = 1$ correspond to the unit triangle and generator, respectively. At stage n of construction the generator is enlarged 2^n times and each of its three upward oriented triangular segments is filled with the structure at stage $(n-1)$.

Luscombe and Desai [17] showed that, for nonzero magnetic field, four parameters are needed to obtain exact RG recursive relations. In their derivation of these relations they use partial partition functions Z_1, Z_2, Z_3 and Z_4, defined at each stage n by fixing

the three apex spins into configurations $\{+,+,+\}$, $\{+,+,-\}$, $\{+,-,-\}$ and $\{-,-,-\}$, respectively, and by performing the summation over all possible configurations of all the other spins. Since we are interested in the partition function itself, rather than the fixed points of the RG transformations, we can regard Z_1, Z_2, Z_3 and Z_4 as the RG parameters. Thus, denoting by Z_i' $\{i = 1,\ldots,4\}$ the partial partition functions at stage $n+1$, and using a slightly different approach [18] than Luscombe and Desai [17], we obtain the following RG recursion relations:

$$\begin{aligned}
Z_1' &= Z_1^3 y^{-3} + 3Z_1 Z_2^2 y^{-1} + 3Z_2^2 Z_3 y + Z_3^3 y^3 ,\\
Z_2' &= Z_1^2 Z_2 y^{-3} + 2Z_1 Z_2 Z_3 y^{-1} + 2Z_2 Z_3^2 y + Z_2^2 Z_4 y\\
&\quad + Z_3^2 Z_4 y^3 + Z_2^3 y^{-1} ,\\
Z_3' &= Z_1 Z_2^2 y^{-3} + 2Z_2^2 Z_3 y^{-1} + 2Z_2 Z_3 Z_4 y + Z_1 Z_3^2 y^{-1}\\
&\quad + Z_3 Z_4^2 y + Z_3^3 y ,\\
Z_4' &= Z_2^3 y^{-3} + 3Z_2 Z_3^2 y^{-1} + 3Z_2^2 Z_4 y + Z_4^3 y^3 ,
\end{aligned} \tag{9}$$

where $x \equiv \exp(\beta J)$ and $y \equiv \exp(\beta H)$. The total partition function at stage n is given by

$$Z = Z_1 + 3Z_2 + 3Z_3 + Z_4 . \tag{10}$$

Hence, starting with partial partition functions for the unit triangle ($n = 0$)

$$\begin{aligned}
Z_1^{(0)} &= x^3 y^3 ,\\
Z_2^{(0)} &= x^{-1} y ,\\
Z_3^{(0)} &= x^{-1} y^{-1} ,\\
Z_4^{(0)} &= x^3 y^{-3} ,
\end{aligned} \tag{11}$$

the stage n partition function is obtained by applying recursion relations (9) n times, and then using (10). The terms of the resulting expression for Z will have the general form $\lambda x^{\mu} y^{\nu}$ (where λ, μ and ν are integers), that is, Z itself will be of the form (2). Although the above procedure is conceptually simple (it consists of multiplication and addition of polynomials in x and y), it cannot be implemented easily for increasing n. To surmount this problem, we implemented the underlying procedure numerically [16], to obtain the DOS functions up to stage 4 of construction of the lattice.

3.3. *Comparison between different geometries*

To display the rapid convergence of the DOS surfaces towards the corresponding limiting surfaces, in Fig. 2 we depict the data for different system sizes for the triangular lattice, the linear chain and the Sierpinski gasket. The corresponding pictures for the square lattice DOS surfaces are given in Ref. [9]. It can be seen from Fig. 2 that in all cases under study the convergence of the DOS functions is manifested through the rapid smoothing of the surfaces with increasing system size, while their shape remains basically unchanged. This means that, although the systems are rather small,

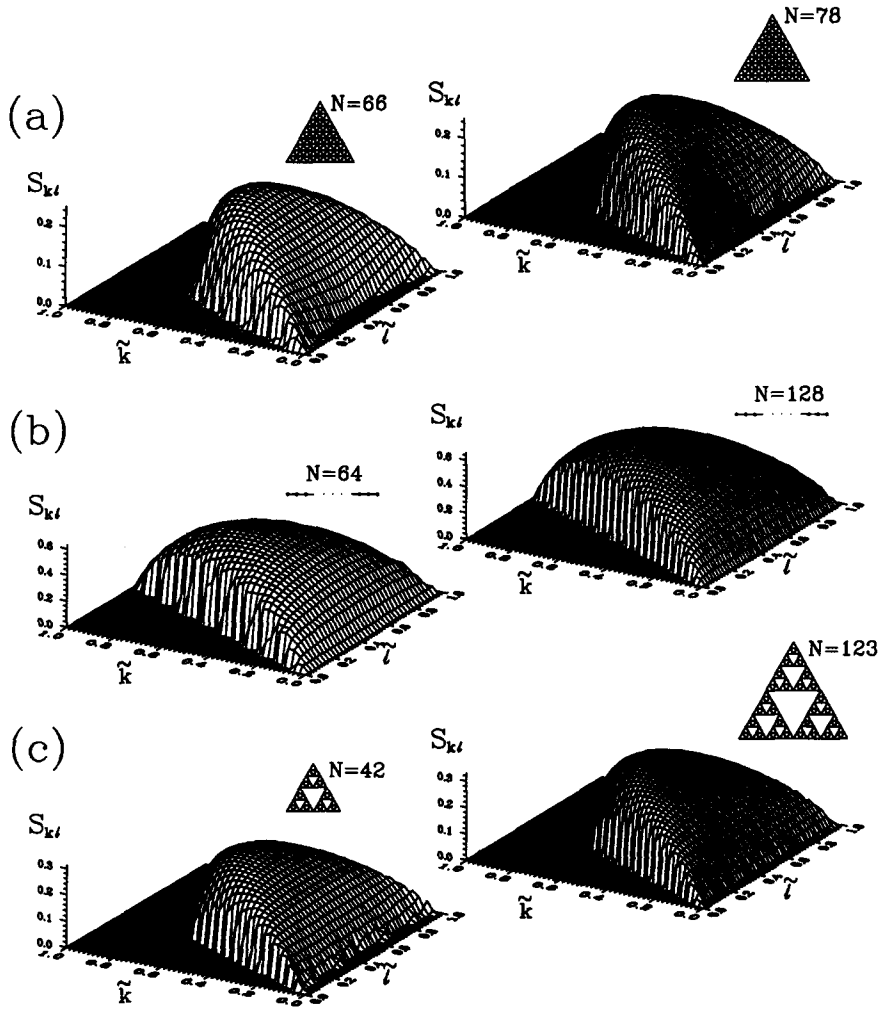

Fig. 2. The scaled DOS surfaces $S_{k\ell}$ presented versus scaled interaction energy variable $\tilde{k} \equiv k/N_B$ and scaled magnetization variable $\tilde{\ell} \equiv \ell/N$, for the Ising model on (a) the equilateral wedge of the triangular lattice with 11 and 12 spins in the base, (b) the linear chain with $N = 64$ and $N = 128$ spins, and (c) the Sierpinski gasket at the 3rd and 4th stage of its construction. In all three cases we observe rapid convergence of the surfaces with increasing system size, towards stable shapes that can be expected for infinite systems.

their DOS surfaces rapidly approach the stable shapes that can be expected for the corresponding infinite system. In particular, we note the clear appearance (see Fig. 2) of flat regions of the DOS functions, where $\mathscr{D}_{k\ell} = 0$ (and, for practical reasons, we denote also $\mathscr{S}_{k\ell} = 0$), together with the fact that their shapes do not change appreciably with increasing system size. The boundaries of these regions separate accessible and inaccessible states of the system under study, and so represent the limits of phase stability.

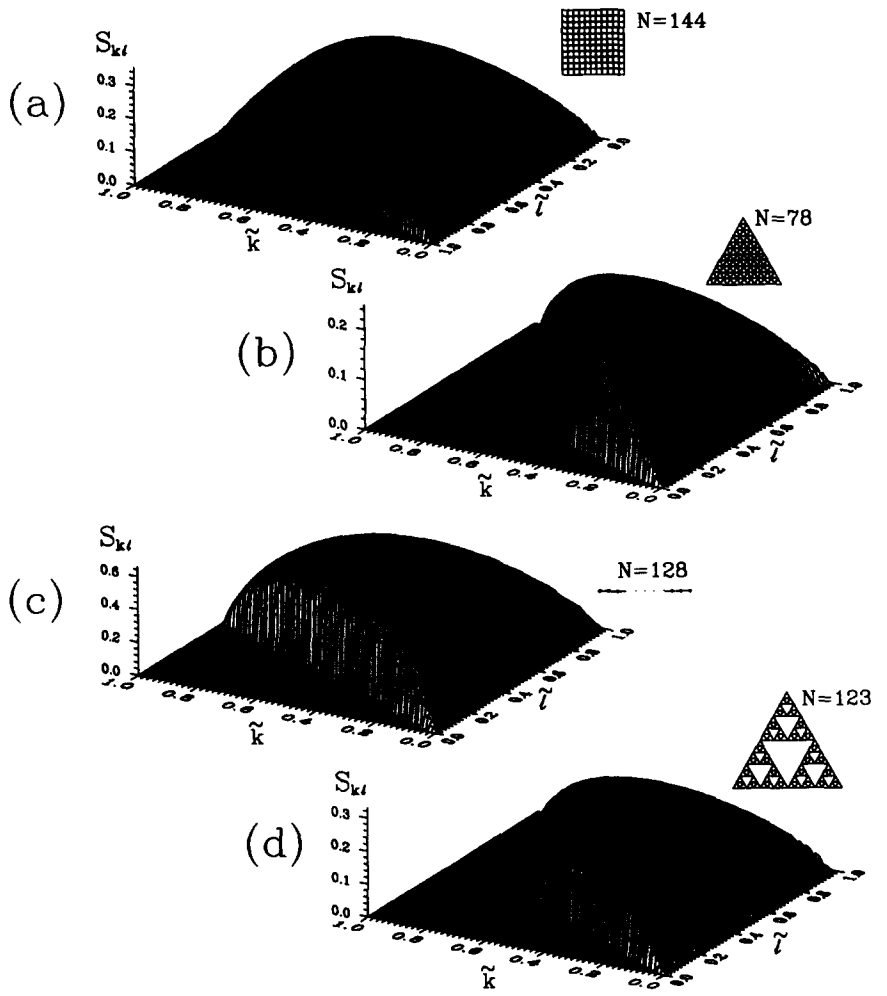

Fig. 3. Comparison of the scaled DOS surfaces for the Ising systems on (a) the square lattice with 12×12 spins, (b) the wedge of the triangular lattice with 12 spins in the base, (c) the linear chain with $N = 128$ spins, and (d) the Sierpinski gasket at the stage 4 of its construction. Note that at small energies (small $\tilde{k}$) the DOS surfaces are convex around zero magnetization ($\tilde{\ell} = 0.5$) for the square and triangular lattices.

To compare the DOS functions for different lattices, we show in Fig. 3 the DOS surfaces for the largest systems for which we have performed calculations:

(i) the square lattice with 12×12 spins,

(ii) wedge of the triangular lattice with 12 spins in the base,

(iii) linear chain with 128 spins, and

(iv) the Sierpinski gasket at the stage 4 of its construction.

While making this comparison, we keep in mind the fact that the Ising ferromagnet on both the square and triangular lattice has spontaneous magnetization for $T \neq 0$, which is not true in the case of the chain and the gasket.

We first observe from Fig. 3 that the DOS surfaces for the square and triangular lattices are convex (with respect to $\tilde{\ell}$) for small $\tilde{k}$, while the surfaces for the chain and gasket are concave. At low temperatures, the dominant states are those with low energies.

(a) When the DOS surface is *convex* at low energies, states with finite magnetization will have the maximum degeneracies, at a given low-energy cross-section of the DOS function. Thus, the equilibrium state of the system will be given by one of these maximum degeneracy states with finite magnetization. This explains why the convexity of the DOS surface results in a finite spontaneous magnetization.

(b) When the DOS surface is *concave*, the equilibrium properties of the system are always determined by states with zero magnetization, and we do not observe a phase transition.

The concavity of the Sierpinski gasket DOS surface is expected to occur for all fractals with a finite order of ramification. This concavity is determined by the number of spin configurations that can be realized for small values of energy (small percentage of unsatisfied bonds) and small values of magnetization (roughly half of the spins "up" and half of the spins "down"). For a small value of energy, if the number of spin configurations with small magnetization is larger than or comparable to the number of configurations with larger magnetization, then the DOS function will be concave. Otherwise, it will be convex. Starting with a configuration with all spins "up", it is possible in the case of the chain and in the case of finitely ramified fractals to destroy the nonzero magnetization at a very small energy cost. This can be done trivially for the chain since the spins of any arbitrary segment of the chain can be flipped, with only the spins at the edges of the segment unfavorably aligned. In the case of a finitely ramified fractal, a finite number of links connect any arbitrarily large part of the lattice with the rest of the lattice. Hence the total magnetization of the fractal lattice can be changed dramatically without affecting the energy significantly. To establish the concavity of the DOS function, however, it is necessary to show that the degeneracies at low energies decrease with increasing magnetization. Although a general argument is difficult to make, for individual cases that have been studied [18] the DOS surfaces are concave at low energies. In the case of compact Euclidean lattices and infinitely ramified fractals, however, one can flip a large part of the lattice only by simultaneously upsetting a large number of bonds (the interface between the two parts corresponds to the linear size of the system).

3.4. *Existence of spontaneous magnetization*

It was shown in Section 2 that the "free energy" minima can be located as the points of maximum difference between the DOS surface and the plane $-2\beta(\tilde{k}J+\tilde{\ell}(N/N_B)H)$. In Fig. 4(a), this procedure is depicted for the zero field ferromagnet on the square lattice, being well above the system critical temperature ($k_BT_c = 2/[\ln(1+\sqrt{2})]$ [1]) where both the DOS surface and the $-2\beta\tilde{k}J$ plane are shown. Changing temperature

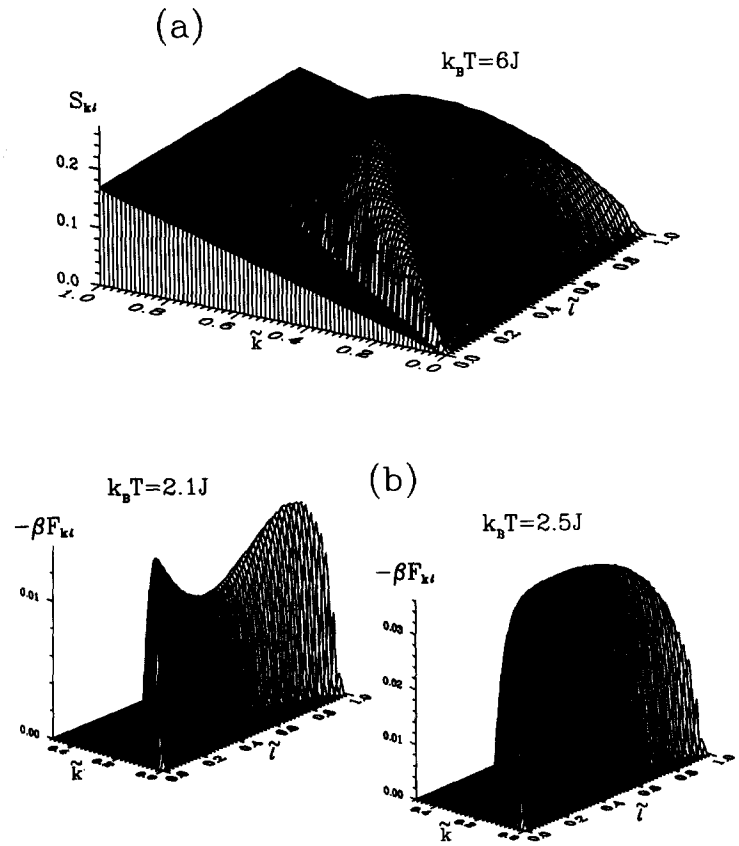

Fig. 4. (a) The DOS surface for the Ising system on the square lattice with 12×12 spins, and the plane defined by $-2\beta(\tilde{k}J + \tilde{\ell}(N/N_B)H)$ (see Eq. (7)), for the choice of parameters $1/\beta = 6J$ and $H = 0$. The difference between the DOS surface and the plane determines the negative "free energy" $-\beta F_{k\ell}$. (b) The negative "free energy" for the same system as in (a), for $H = 0$ and two different choices of temperature. The appearance of the saddle-point at lower temperatures implies the existence of spontaneous magnetization.

corresponds to changing the angle of rotation of the plane about the $\tilde{\ell}$ axis, while changing the field corresponds to rotation about the $\tilde{k}$ axis.

In Fig. 4(b) we present the surface $-\beta F_{k\ell}$ for the same system, for different temperature values. Below the critical temperature, there are two distinct peaks corresponding to nonzero positive and negative spontaneous magnetization values, whereas above T_c there is just one peak corresponding to zero magnetization. Notice that the peaks of the "free energy" surface for temperatures below T_c correspond to the ridges of the DOS surface, which can thus be related to the zero field equilibrium magnetization values. In addition, one can observe that introducing nonzero field (that is, rotating the plane $-2\beta\,\tilde{k}J$ around the $\tilde{k}$ axis) breaks the symmetry (with respect to the $\tilde{\ell} = 0.5$ plane) of the peaks of the $-\beta F_{k\ell}$ surface. In Fig. 5 we present the $-\beta F_{k\ell}$ surfaces for the triangular lattice, the linear chain and the Sierpinski gasket in zero field, from which

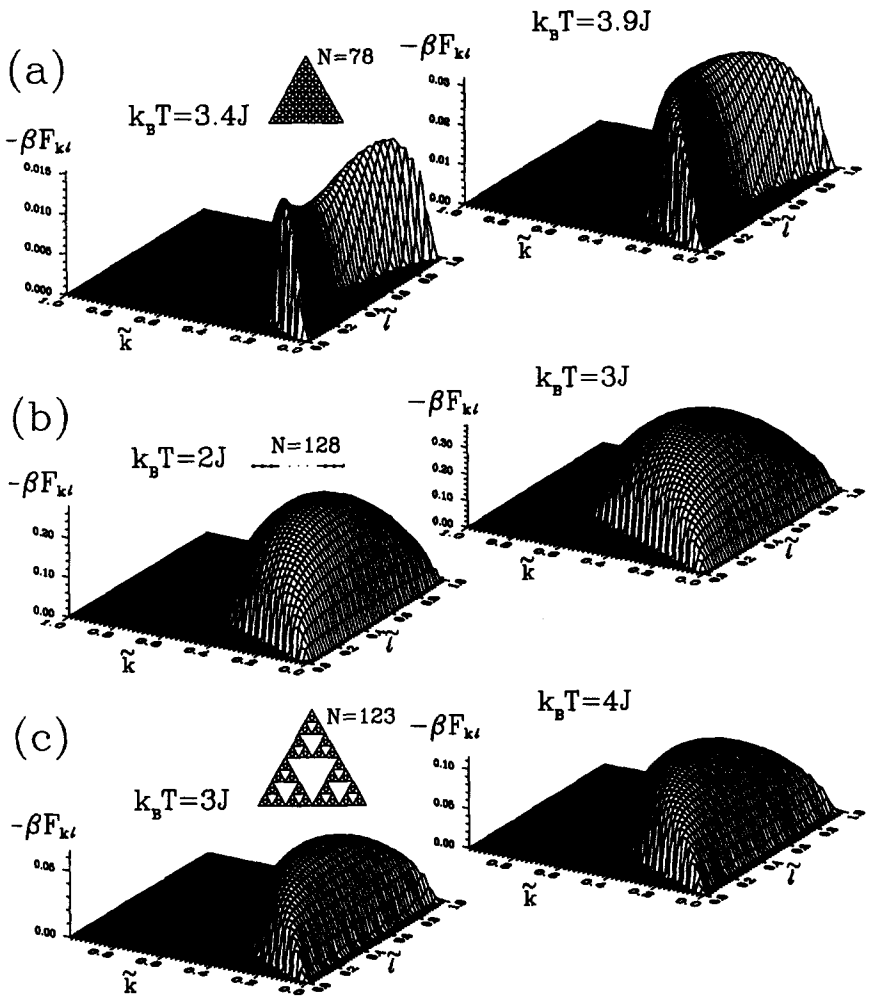

Fig. 5. The negative "free energy" as given by the term in square brackets in Eq. (7), for the Ising systems (at various temperatures, and in zero field) (a) on the equilateral wedge of the triangular lattice with 12 spins in the base, (b) the linear chain with $N = 64$ spins, and (c) the Sierpinski gasket at the stage 4 of its construction. The presence of two peaks at $\tilde{\ell} \neq 0.5$ in the first surface for the triangular lattice indicates spontaneous magnetization below T_c.

it is evident that only the triangular lattice exhibits spontaneous magnetization at low temperatures.

4. DOS Functions for the Ising model with next-nearest-neighbor interactions

The presence of both the nearest-neighbor (*nn*) and the next-nearest-neighbor (*nnn*) interactions for the Ising model on the square lattice introduces more complex

thermodynamic behavior [19]. It offers a challenge for the application of the DOS function approach, and here we study the Ising model for different ratios of the two interaction parameters.

4.1. Definitions

We now consider the Hamiltonian

$$\mathscr{H} = -J_1 \sum_{\langle nn \rangle} s_i s_j - J_2 \sum_{\langle nnn \rangle} s_i s_j - H \sum_i s_i \,, \tag{12}$$

where $\langle nnn \rangle$ denotes summation over next-nearest-neighbor pairs, J_1 is the *nn* interaction strength and J_2 is the *nnn* interaction strength. The analog of Eq. (3) for the partition function for the system with N spins, connected by N_{B_1} nearest-neighbor bonds and N_{B_2} next-nearest-neighbor bonds, is given by

$$Z = \exp\{\beta(J_1 N_{B_1} + J_2 N_{B_2} + HN)\} \sum_{k_1=0}^{N_{B_1}} \sum_{k_2=0}^{N_{B_2}} \sum_{\ell=0}^{N} \mathscr{D}_{k_1 k_2 \ell} \times \exp\{-2\beta(k_1 J_1 + k_2 J_2 + \ell H)\} \,, \tag{13}$$

where $\mathscr{D}_{k_1 k_2 \ell}$ are degeneracies of discrete energy levels

$$E_{k_1 k_2 \ell} = J_1(-N_{B_1} + 2k_1) + J_2(-N_{B_2} + 2k_2) + H(-N + 2\ell) \,, \tag{14}$$

while integers k_1 $(0 \leqslant k_1 \leqslant N_{B_1})$ and k_2 $(0 \leqslant k_2 \leqslant N_{B_2})$ represent the number of *nn* and *nnn* bonds with antiparallel spins at their ends, respectively.

It is clear that the interaction energy scale, determined by the first two terms on the right-hand side of (14), now depends on the choice of the ratio $R \equiv J_1/J_2$. In order to compare the DOS functions for different values of R, we introduce a general interaction energy scale

$$\tilde{\mathscr{E}}_{k_1 k_2} = \frac{[J_1(-N_{B_1} + 2k_1) + J_2(-N_{B_2} + 2k_2) - E_{\min}]}{E_{\max} - E_{\min}} \,, \tag{15}$$

where $E_{\min}$ and $E_{\max}$ are the minimum and the maximum value, respectively, of the interaction energy term $J_1(-N_{B_1} + 2k_1) + J_2(-N_{B_2} + 2k_2)$, for a given choice of J_1 and J_2. The interaction energy $\tilde{\mathscr{E}}_{k_1 k_2}$ takes values in the interval $[0, 1]$, for all choices of k_1, k_2, J_1 and J_2. For extremely large (or small) values of R, the energy scale is divided into main levels (determined by the stronger interaction) and closely spaced sublevels (determined by the weaker coupling). It is helpful to bin the energy scale into equidistant intervals (we choose the number of intervals to be proportional to the number of main levels). Whether the energy scale is binned or not, for each particular choice of J_1 and J_2, the energy levels are organized in increasing order, so that the possible interaction energy values are given by the set $\{\mathscr{E}_k;\ k = 1, \ldots, N_L\}$, with $\mathscr{E}_k < \mathscr{E}_{k'}$ for $k < k'$. Here $N_L \leqslant (N_{B_1} + 1)(N_{B_2} + 1)$ is either the number of possible combinations of indices k_1 and k_2 (that label distinct energy levels), if the scale is not binned, or the number of the energy intervals, if the scale is binned. The corresponding

degeneracies, in case of binning, are sums of degeneracies of the actual levels found inside a given interval (bin). The entropy $\mathscr{S}_{k\ell}$ per spin is given by

$$\mathscr{S}_{k\ell} \equiv \frac{\ln \mathscr{D}_{k\ell}}{N}, \tag{16}$$

corresponding to the energy level

$$E_{k\ell} \equiv [\mathscr{E}_k (E_{\max} - E_{\min}) + E_{\min}] + H(-N + 2\ell). \tag{17}$$

Hence, the partition function can be written in the form

$$Z = e^{\beta(-E_{\min}+HN)} \sum_{k=0}^{N_L} \sum_{\ell=0}^{N} \exp\left\{N\left[-\beta\left(\mathscr{E}_k \frac{E_{\max} - E_{\min}}{N} + 2\tilde{\ell}H\right) + \mathscr{S}_{k\ell}\right]\right\}, \tag{18}$$

which is the analog of (8) for the *nn* interaction case. Further analysis of the DOS function (16), plotted versus scaled energy variable $\mathscr{E}_k$ and scaled magnetization variable $\tilde{\ell}$, *for each particular choice* of J_1 and J_2, is analogous to the *nn* case analysis which has been performed in Section 3.

Before going into details, we note that the DOS function is determined only by the topology of the lattice and the ratio R. Similar to the *nn* case, where the possible states of the ferromagnet and the antiferromagnet correspond to different parts of the DOS surface, for given $R > 0$ the region $\mathscr{E}_k \leqslant 0.5$ corresponds to the case with $(J_1 > 0)$ and $(J_2 > 0)$, and $\mathscr{E}_k \geqslant 0.5$ corresponds to the case with $(J_1 < 0)$ and $(J_2 < 0)$. On the other hand, for given $R < 0$ the $\mathscr{E}_k \leqslant 0.5$ region corresponds to $(J_1 < 0)$ and $(J_2 > 0)$ and $\mathscr{E}_k \geqslant 0.5$ corresponds to $(J_1 > 0)$ and $(J_2 < 0)$.

Using the TM method [9] generalized for the present case of *nn* and *nnn* interactions, we obtain [16] exact data $\{\mathscr{D}_{k_1 k_2 \ell}; k_1 = 0, \ldots, N_{B_1}; k_2 = 0, \ldots, N_{B_2}; \ell = 0, \ldots, N\}$ for the square lattice with up to 9×9 spins. In Figs. 6 and 7 we present the DOS surfaces of the system with 9×9 spins for five positive and five negative representative values of R, respectively. The first overall observation is that the variation of the ratio R causes larger differences in the shape of DOS functions than the variation of the underlying lattices in the *nn* case (see Fig. 3). In the next two paragraphs we shall comment separately on the positive and negative R cases.

4.2. *R-dependent behavior*

Starting with a very small positive value of R, when the two ferromagnetic sublattices are almost decoupled, we can notice from Fig. 6 that there are three ridges of the DOS surface that occur at small values of $\mathscr{E}_k$ and $\tilde{\ell} \sim 0$, $\tilde{\ell} \sim 0.5$ and $\tilde{\ell} \sim 1$, whose initial parts correspond to the $\{+,+\}$, $(\{+,-\};\{-,+\})$ and $\{-,-\}$ configurations of the sublattices, respectively. The beginning of the middle ridge is shifted slightly forward on the energy scale (in comparison with the outer ridges). Looking from the opposite side (corresponding to $(J_1 < 0)$ and $(J_2 < 0)$), we find that the single central ridge is also slightly shifted away from $\mathscr{E}_k = 1$, indicating a slight frustration of the system at low temperatures (without macroscopic residual entropy). When R is increased, the

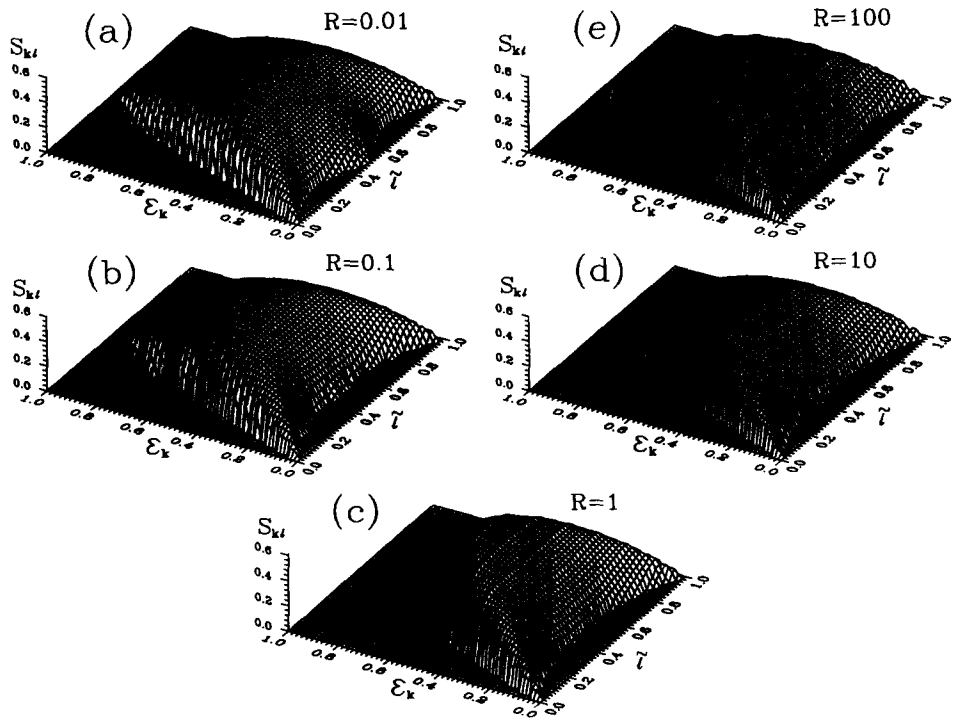

Fig. 6. The DOS surfaces for the square Ising model with 9×9 spins, with the *nn* and *nnn* interactions, for various positive values of the ratio $R \equiv J_1/J_2$. The diversity of the DOS function shapes is much greater than in the case of the *nn* Ising model situated on different lattices.

central ridge is further shifted forward on the energy scale until it totally disappears at $R = 1$ while, at the same time, the frustration of the antiferromagnetic case increases. The sharp cutoff of the DOS function, at large $\mathcal{E}_k$, for $R = 1$, indicates the appearance of a nonzero residual entropy of the corresponding antiferromagnet; the ground state energy level is highly degenerate. Further increasing R reduces the frustration, and for $R \gg 1$ the effect of the presence of *nnn* interactions becomes negligible (one can compare the $R = 100$ DOS surface with the surface depicted in Fig. 3(a)).

For small negative values of R the situation is similar to that observed in the case of small positive R, except that now the two outer ridges, compared with the middle ridge for small $\mathcal{E}_k$, are shifted forward on the energy scale (see Fig. 7). This is related to the fact that the two almost decoupled ferromagnetic sublattices mutually interact through weak antiferromagnetic coupling, and the ground state of the system corresponds to the Néel spin configuration. On the other hand, the shape of the DOS surface on the large $\mathcal{E}_k$ side again shows slight frustration of the spin system, corresponding to the fact that if both sublattices order antiferromagnetically (large $|J_2|$) then the weak ferromagnetic *nn* bonds (that connect the sublattices) cannot all be simultaneously satisfied. Increasing the magnitude of R shifts the two outer ridges still forward, on the energy scale, up to

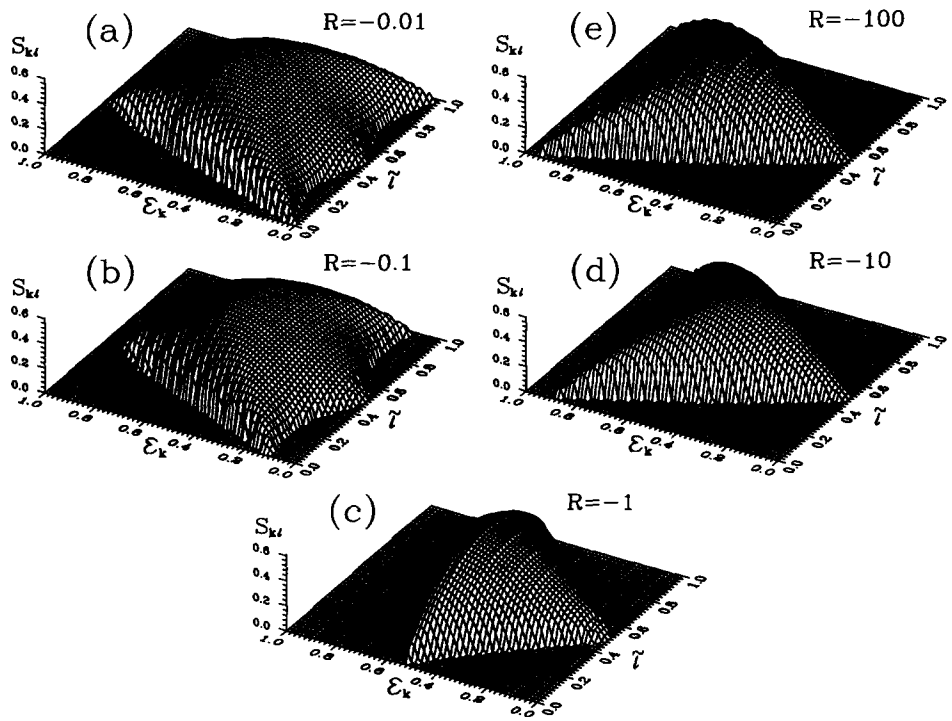

Fig. 7. The DOS functions for the same system as in Fig. 6, for various negative values of the ratio R.

the point $\mathcal{E}_k = 0.5$, for $R = 1$. At the same time, looking from the large $\mathcal{E}_k$ side, the frustration is increased and residual entropy is brought about. If the magnitude of R is further increased and the antiferromagnetic *nn* coupling takes over, only the central ridge remains on the small $\mathcal{E}_k$ side. The large $\mathcal{E}_k$ side [$(J_1 > 0)$ and $(J_2 < 0)$] now becomes more interesting, since the two outer wedges take over the role of ground states and the residual entropy is destroyed, although the system remains frustrated (in the sense that the *nnn* bonds are not satisfied in the ground state spin configurations). Finally, for $R \ll 0$ we again arrive at the already observed *nn* limit (see Fig. 3(a); in fact, the DOS function depicted in Fig. 8(e) represents the mirror image of the DOS function in Fig. 7(e)).

4.3. *First order transitions*

We conclude this section by demonstrating that the DOS function approach can be used not only as a graphical tool for detecting the continuous appearance (disappearance) of spontaneous magnetization, but also as a tool for studying abrupt changes of magnetization. We shall show this in the case of a metamagnet $(J_1 < 0)$ and $(J_2 > 0)$ in (12) [19]. The metamagnet can display either a first- or a second-order phase transition between the paramagnetic phase and the antiferromagnetic phase depending on the

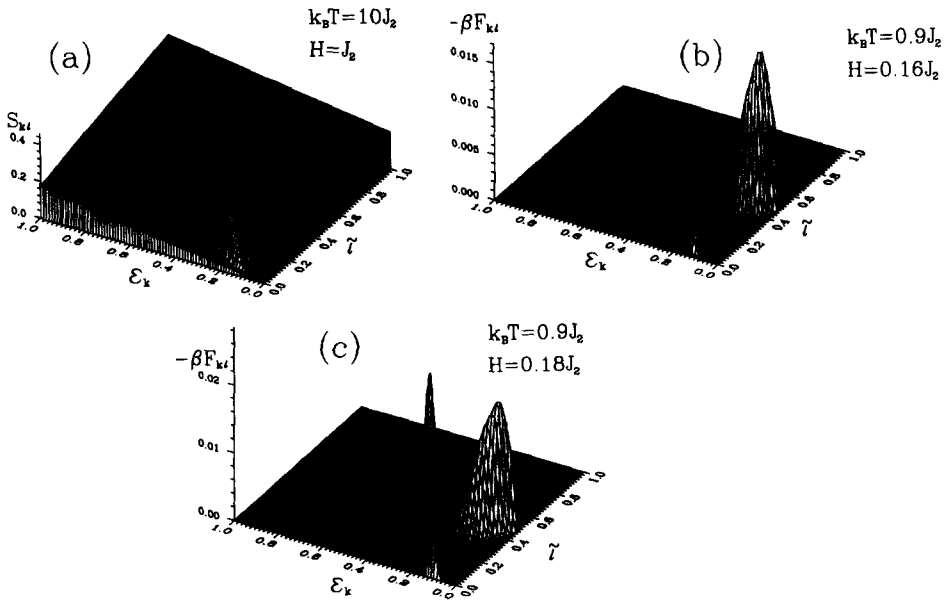

Fig. 8. The graphic demonstration of the existence of the first-order phase transition in the case of the metamagnet represented by the model Hamiltonian (11), with $J_1/J_2 = -0.1$. (a) The DOS surface for the 9×9 system cut by the plane $-\beta[\mathscr{E}_k(E_{\max} - E_{\min})/N + 2\tilde{\ell}H]$ (see Eq. (16)), for the choice $1/\beta = 10J_2$ and $H = J_2$. (b) The negative "free energy" surface at $1/\beta = 0.9J_2$ and $H = 0.16J_2$. (c) The same surface as in (b) for $H = 0.18J_2$. In (b), the peak at low magnetization is higher than the high magnetization peak. A small increase in H causes the high magnetization peak to become dominant, in (c).

temperature, at finite values of the field H. We have already drawn the DOS functions of such systems in Fig. 7. A typical example is the case $R = -0.1$ (see Fig. 7(b)). To observe the first-order transition and obtain the value of the field at which it happens, we calculate the "free energy surface" as described in Section 3 for the *nn* Ising case. For each set of values of T and H, we subtract the plane $-\beta[\mathscr{E}_k(E_{\max} - E_{\min})/N + 2\tilde{\ell}H]$ from the DOS surface, and search for the maximum value of the resulting surface (see Eq. (16)). The subtraction is depicted in Fig. 8(a) for $R = -0.1$. Figs. 8(c) and (d) show the negative of the "free energy" for two values of H separated by a first-order line, for a fixed value of temperature. For the lower value of the field, the maximum of the negative "free energy" appears at a very low magnetization (Fig. 8(b)), which is abruptly shifted to a high magnetization (Fig. 8(c)) for the higher field value.

We use this procedure at different temperatures below the tricritical temperature to locate magnetic field values for which the first-order transition occurs. As in the *nn* case, we identify the corresponding magnetization values by locating the peak positions of the "free energy surface". Above the tricritical temperature, the "free energy surface" exhibits a single peak at all fields, since the transition from the paramagnetic state to the antiferromagnetic state is of second order. The magnetization at the second-order transition exhibits a discontinuous slope. We use this as the criterion for locating the field values at which the second-order transitions take place.

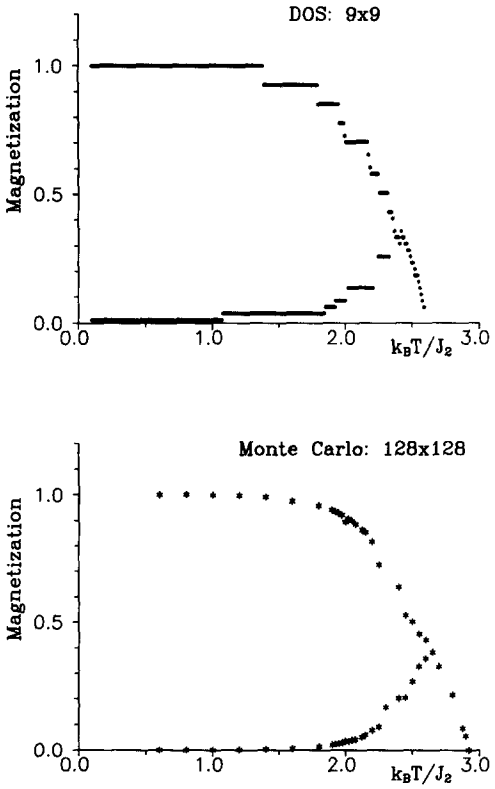

Fig. 9. The phase diagram of the metamagnet represented by the model Hamiltonian (11), with $J_1/J_2 = -0.1$ obtained using the procedure described in Fig. 8 from DOS functions of a 9×9 system, together with the corresponding phase diagram obtained from Monte Carlo simulations of a 128×128 system. While the phase diagram obtained from the DOS functions exhibits pronounced finite size effects, it still gives a fair representation of the infinite system behavior. In conjunction with the more accurate (but time consuming) Monte Carlo method, this approach may be used for preliminary analysis of system behavior for a wide range of parameters (such as the interaction ratio in the present case of the metamagnet).

In Fig. 9 we show the magnetization values at the first- and second-order transitions obtained from the procedure described. In Fig. 9 we also show the phase diagram obtained from Monte Carlo simulations of a 128×128 system. We see that the phase diagram obtained from the DOS functions gives a fair representation of infinite size behavior, as obtained by the Monte Carlo data.

While the Monte Carlo method provides more accurate results, the DOS functions can be very useful in exploring wide parameter ranges. The DOS functions are calculated without reference to specific values of the interactions. With minimal additional computational effort, the *same* DOS function can be used for analysis of behavior in different regimes of parameter values. Thus, for models with multiple parameters, the DOS function calculations may be used in conjunction with Monte Carlo calculations to explore overall behavior.

5. Conclusions

We have presented exact enumerations of the density of states functions of Ising systems with *nn* couplings in *nonzero* field, for the square lattice (up to size 12×12), the triangular lattice (having up to 12 spins in the base), linear chain (having up to $N = 128$ spins), and the Sierpinski gasket (up to stage 4). We also presented the density of states functions (DOS) for the square lattice with *nn* and *nnn* interactions, in nonzero field, with 9×9 spins.

Analyzing the scaled DOS functions for systems with *nn* interactions on various lattices, we found that the topology of the lattice alone determines the shape of the DOS surface. In all cases where the model exhibits nonzero spontaneous magnetization at nonzero temperatures, the DOS functions are convex in the low interaction energy region. A simple graphic construction was then used to determine the regions of interaction energy and magnetization that correspond to the equilibrium states at different values of temperature and field. When both the *nn* and *nnn* interactions are present, the interaction energy scale depends on the ratio $R \equiv J_1/J_2$, resulting in different DOS functions for different values of R. In this case, the DOS surfaces differ from one another more than the DOS surfaces for systems with *nn* interactions situated on different lattices. We studied the DOS surfaces for different positive and negative values of R.

We demonstrated the existence of first-order phase transitions at finite magnetic field by studying the "free energy surface" obtained from the DOS surface, for different temperature and magnetic field values. We obtained the phase diagram of the system for a specific value of R using this method, and suggested how DOS function calculations may be used in exploring the behavior of systems in a complementary fashion to the well-established Monte Carlo method. In an alternate approach of using DOS function calculations to study critical phenomena, series expansions coefficients to large orders have recently been obtained from finite lattice calculations [20].

We note that our approach has some features in common with the "histogram Monte Carlo" approach [21]. These approaches are similar in that it is not necessary to make a new calculation for each set of parameters. For example, if one makes a Monte Carlo calculation of the specific heat for one temperature, then using the histogram approach, one can obtain the specific heat for nearby temperatures without requiring additional Monte Carlo calculations. In our method, a single calculation of the DOS functions suffices to obtain the specific heat for all temperature values (not only nearby temperatures). The advantage of the histogram Monte Carlo method is that large system sizes can be treated, while the advantage of our method is that it gives the full phase diagram.

Acknowledgements

We thank A.-L. Barabasi, S. Havlin, S. Schwarzer, T. Stošić and especially H. Larralde for helpful discussions and comments on the manuscript. SS thanks Robert

Putnam of Thinking Machines Corp. for help in computations done on the CM-2, and the Center for Computational Physics at Boston University for computational facilities. This work has been supported in part by the NSF, CNPq (Brazilian Agency), the Yugoslav–USA Joint Scientific Board under project JF900 (NSF), and the Serbian Science Foundation under project 0103.

References

[1] C. Domb, Adv. Phys. 9 (1960) 165.
[2] H.E. Stanley, Introduction to Phase Transitions and Critical Phenomena (Oxford University Press, Oxford, 1971).
[3] S.K. Ma, Modern Theory of Critical Phenomena (W.A. Benjamin, Reading, MA, 1976).
[4] C. Domb, in: Phase Transitions and Critical Phenomena, Vol. 3, eds. C. Domb, M.S. Green (Academic Press, New York, 1972).
[5] K. Binder, D. Heermann, Monte Carlo Simulation in Statistical Physics (Springer, Berlin, 1988).
[6] R.J. Baxter, F.Y. Wu, Phys. Rev. Lett. 31 (1973) 1294.
[7] M.T. Jaekel, J.M. Maillard, J. Phys. A 18 (1985) 1229.
[8] F.Y. Wu, J. Statist. Phys. 40 (1985) 613.
[9] B. Stošić, S. Milošević, H.E. Stanley, Phys. Rev. B 41 (1990) 11 466.
[10] Here we distinguish, for the sake of clarity, two terms: magnetization and equilibrium magnetization where the former refers to magnetization of one particular spin configuration of a finite system, and the latter refers to the magnetization that the corresponding infinite system can have in an equilibrium state.
[11] K. Huang, Statistical Mechanics (Wiley, New York, 1963).
[12] S. Ono, Y. Karaki, M. Suzuki, C. Kawabata, J. Phys. Soc. Japan 25 (1968) 54; M. Suzuki, C. Kawabata, S. Ono, Y. Karaki, M. Ikeda, J. Phys. Soc. Japan 29 (1970) 837.
[13] K. Binder, Physica 62 (1972) 508.
[14] G. Bhanot, S. Sastry, J. Stat. Phys. 60 (1990) 333.
[15] C.N. Yang, T.D. Lee, Phys. Rev. 87 (1952) 101.
[16] The DOS functions presented here were calculated on IBM RS6000 workstations and the Connection Machine CM-2. For the 12×12 *nn* square lattice, the calculations required runs of about 2 h on the CM-2 using 16 384 processors (with 64K of memory each) and about 4 h of data manipulation runs using Mathematica on a DECstation 5000 Model 240. For the 9×9 *nnn* square lattice, the calculations required runs of about 6 h on the CM-2 using 16 384 processors (with 128K of memory each) and about 12 h of data manipulation runs using Mathematica on a DECstation 5000 Model 240. The calculations for the wedge of the triangular lattice with 12 spins in the base required 7 h CPU time on the IBM RS6000, using 380Mb of virtual memory, and the calculations for stage 4 of construction of the Sierpinski gasket (with altogether 128 spins) required 15 h CPU time.
[17] J.H. Luscombe, R.C. Desai, Phys. Rev. B 32 (1985) 1614.
[18] T. Stošić, B. Stošić, S. Milošević, H.E. Stanley, preprint.
[19] I.D. Lawrie, S. Sarbach, in: Phase Transitions and Critical Phenomena, Vol. 9, eds. C. Domb and J.L. Lebowitz (Academic Press, New York, 1984); E. Stryjewski and N. Giordano, Adv. Phys. 26 (1977) 487.
[20] G. Bhanot, M. Creutz and J. Lacki, Phys. Rev. Lett. 69 (1992) 1841.
[21] See, e.g., the recent review of R.H. Swendsen, Modern methods of analyzing Monte Carlo computer simulations, Proc. STATPHYS-18, Physica A 194 (1993) 53, and references therein.